

Comparative Study of Ultrasound and Magnetic Resonance Imaging of Adnexal Masses

Narikelapu Nitya¹, Rama Krishna Rao Baru²

¹Post Graduate, Department of Radio-Diagnosis, Narayana Medical College & Hospital, Nellore, Andhra Pradesh, India, ²Professor, Department of Radio-Diagnosis, Narayana Medical College & Hospital, Nellore, Andhra Pradesh, India.

Abstract

Background: Current study aimed to assess the role of ultrasound and MRI in the evaluation of adnexal mass lesions and comparison with clinical outcomes. **Subjects & Methods:** A total of 30 suspected adnexal mass detected on ultrasonography was performed MRI, and accuracy of both USG and MRI were compared with histopathology. **Results:** Abdominal pain was predominantly confined to the lower abdomen in 13 of 30 cases (43.3%). On USG total number of benign lesions was 19, and the total number of malignancies was 11. However, on MRI, 21 cases were mild, and 9 cases were malignant. six cases were diagnosed as malignant in ultrasound. In these six cases, two cases were serous cystadenocarcinoma, two were mucinous cystadenocarcinoma, one was serious papillary cystadenocarcinoma of the fallopian tube, and one was a malignant tubo-ovarian mass. MRI accurately diagnosed 4 indeterminate cases that correlated with the histopathology report. 9 malignant lesions were diagnosed as malignant by MRI were 3 cases of serous cystadenocarcinoma, 2 cases of mucinous cystadenocarcinoma, 1 case of malignant tubo-ovarian mass, 1 case of endometrioid carcinoma, 1 case of serous papillary cystadenocarcinoma of the fallopian tube and 2 cases of malignant sex cord-stromal neoplasms. Both the cases of serous cystadenomas were correctly diagnosed as benign lesions on both ultrasound and MRI. There were 2 cases of mucinous cystadenocarcinoma, which were accurately diagnosed as malignant on both USG and MRI due to the presence of solid components, mural thickening. The sensitivity, specificity, and accuracy of USG were 36.6%, 94% and 55% respectively. The sensitivity, specificity, and accuracy of MRI were 81.80%, 94.7%, and 65.7%, respectively. **Conclusion:** The best agreement was observed between MR findings and diagnosis in origin, tissue content, and tissue characteristics. Sonography had a weak correlation in context to the definitive diagnosis for the origin and tissue content of a mass.

Keywords: Spinal Infection, Magnetic Resonance Imaging, Tubercular, Pyogenic.

Corresponding Author: Rama Krishna Rao Baru, Professor, Department of Radio-Diagnosis, Narayana Medical College & Hospital, Nellore, Andhra Pradesh, India.

E-mail: drkdurga60@gmail.com

Received: 25 August 2020

Revised: 02 October 2020

Accepted: 11 October 2020

Published: 31 December 2020

Introduction

The management options range from radical staging surgery for suspected ovarian malignancy, less invasive surgery (laparoscopy) for likely benign tumors, and conservative nonsurgical management.^[1] Since there is a considerable difference between these types of operations, it is essential to make a final diagnosis.

The incidence of women undergoing surgery for adnexal masses ranged from 5 to 10%, in which less than 25% are malignant.

The clinically diagnosed adnexal lesions are, confirmed following an exploratory surgery and histopathological examination. The nature of the adnexal mass, whether benign or malignant, is not evident before the surgical plan.^[2]

Ultrasonography is the first-line investigation to evaluate the suspected adnexal mass. Magnetic resonance imaging helps to characterize the adnexal masses which were not wholly evaluated by ultrasound as it can provide additional information on soft tissue composition of adnexal masses based on specific tissue relaxation times and allows multiplanar imaging to define the origin and extent of pelvic pathology.

MRI provides a comprehensive and detailed view of the anatomy of the uterus. The uterine body is composed of three distinct zones on T2-weighted images: the endometrium, junctional zone, and myometrium. The inner layer consists of the high-signal-intensity endometrium, which varies in width from 1 to 7 mm, depending on the menstrual cycle. It is often not separated from the fluid within the endometrial cavity. The endometrium is sharply delineated from the junctional

zone or basal layer of the myometrium, which is composed of longitudinally oriented smooth muscle cells. The junctional zone is visualized as a low-signal-intensity stripe at the interface of the endometrium and myometrium and should not exceed a thickness of 8 mm. The outer zone represents the stratum vascular of the myometrium. Its signal intensity depends on the phase of the menstrual cycle, but it usually exhibits intermediate signal intensity on T2-weighted images. In postmenopausal women, the outer myometrium displays lower signal intensity, and the junctional zone is often missing or indistinctly visualized.^[3]

After intravenous contrast administration, endometrium and outer myometrium show pronounced contrast enhancement while the junctional zone is of lower signal intensity due to the denser tissue and smaller extracellular volume of distribution of the contrast.^[3]

Anatomic details of the cervix are also best depicted on the T2 weighted image. The cervical canal is lined by the epithelium of the endocervix, where small folds-the plicae palmitate may be visible. The cervix is mainly composed of dense fibrous stroma, resulting in a typically cylindrical or ring-like formation of low signal intensity on T2- weighted images.^[4] A layer of higher signal intensity surrounds it in the outer cervical stroma, which may sometimes be challenging to differentiate from the adjacent parametrium. Strong gadolinium enhancement of cervical mucosa and parametrium is noted, whereas cervical stroma initially shows little enhancement but enhances progressively on delayed-phase images.^[5,6]

Three normal zones of the vaginal and paravaginal tissues are often depicted on the T2W image. The vaginal muscles and collagen-rich submucosal layer appears as a low signal intensity band on T1W and T2W images. Intraluminally, the vaginal mucosa and any endoluminal secretions have low T1 and high T2 signal intensities.

On Sonography, the normal ovary has a relatively homogenous echotexture with a central, more echogenic medulla. Small, well-defined anechoic or cystic follicles may be seen peripherally in the cortex. During the early proliferative period, many follicles that are stimulated by both FSH and luteinizing hormone develop and increase the size until day 8 of the menstrual cycle. On that day, one follicle becomes dominant, increases in size 2.0 to 2.5 cm, and ovulates.

In the majority of women of reproductive age, the ovaries exhibit zonal anatomy on T2- weighted MRI, with the cortex displaying low signal intensity than the central medulla. The peripheral zone contains multiple small cysts presenting different stages of folliculogenesis, corpus luteum cysts, and surface inclusion cysts. Most follicular derivatives have low to intermediate signal intensity on T1- weighted images and very high signal intensity on T2-weighted images due to the

presence of fluid. Follicles are the landmark of ovaries, which are best identified on the T2W image as a cluster of small high signal intensities.^[6]

The current study aimed to evaluate the role of ultrasound and MRI in the diagnosis of adnexal mass lesions and compare with clinical outcome.

Subjects and Methods

The subjects of this study are the patients who get referred to the department of Radiodiagnosis, NMCH with a suspected adnexal mass.

Inclusion criteria

Clinically suspected cases of adnexal mass lesions.

Adnexal mass lesions were observed on ultrasound.

Exclusion criteria

All uterine mass lesions.

Sociologically proved cases of ectopic pregnancy.

Patients who are having a history of claustrophobia.

All Patients who are having a history of metallic implants insertion, cardiac pacemakers, metallic foreign body insitu.

Study area:

This study was conducted at the Department of Radiology of Narayana Medical College and Hospital, Nellore.

Study period: December 2017 to November 2019 (duration of 2 years)

Method of Collection of Data

Data collection:

Ultrasonography of the pelvis was done by Philips HD 11 with the transducer of 2-5Hz, and Transvaginal Ultrasonography was done with the transducer of 4-8 Hz. MRI of the pelvis was done by GE Signa 3 Tesla MRI.

Following sequences recorded:

Axial T1 weighted spin-echo sequence.

Axial T2 weighted fast spin-echo sequence.

Sagittal T2 weighted fast spin-echo sequence.

Coronal T2 weighted fast spin-echo sequence.

Statistics: Data was analysed by student t-test. Descriptive values sensitivity, specificity, positive and negative predictive values, and accuracy were calculated.

Results

In the present study, all the 30 patients underwent Transabdominal Ultrasonography, and Transvaginal Ultrasonography was performed wherever applicable.

This study comprised 18 to 66 years with a mean age of 40.85 years. Benign lesions were found in the age group of 21-30 years, whereas malignant lesions were observed in the age group of 50-70 years.

The common presenting complaints were abdominal pain confined to the lower abdomen, which comprised of 13 of 30 cases (43.3%) followed by abdominal mass/lump 7 cases (23.3%) and abdominal distension 5 cases (16.6%), menstrual irregularity in 5 cases (16.6%).

More number of benign lesions 19 of 30 cases (63.3%) were identified than malignant lesions.

60% of all ovarian tumors and 85% of malignant ovarian neoplasms are ovarian epithelial neoplasms.

Out of 30 cases, 19 cases were benign, and 11 cases were malignant. The maximum number of cases were benign on both USG and MRI.

On USG total number of benign lesions was 19, and the total number of malignancies was 11. However, on MRI, 21 cases were mild, and 9 cases were malignant.

Table 1: USG diagnosis

USG diagnosis	Number (30)	%
Serous cystadenoma	3	10
Mucinous cystadenoma	2	6.66
Serous cystadenocarcinoma	2	6.66
Mucinous cystadenocarcinoma	2	6.66
Fibrothecoma	1	3.33
Tubo-ovarian abscess	2	6.66
Malignant tubo-ovarian mass	1	3.33
Dermoid	1	3.33
Hemorrhagic cyst	3	10
Simple ovarian cyst	2	6.66
Endometriosis	2	6.66
Other solid benign ovarian tumours	2	6.66
Other malignant ovarian tumour	2	6.66
Indeterminate	5	16.6

The maximum number of cases diagnosed by ultrasound were benign lesion.

Out of all the 19 benign cases on USG, one case of pedunculated subserosal fibroid was wrongly diagnosed as a malignant adnexal lesion due to its complex appearance as a solid cystic lesion with increased vascularity and heterogeneous echogenicity of the solid component on USG. However, MRI revealed the exact origin of the mass from the uterus.

Out of 30 cases, six cases were diagnosed as malignant in ultrasound. Out of these six cases, two were serious cystadenocarcinoma, two were mucinous cystadenocarcinoma, one was serious papillary cystadenocarcinoma of the fallopian tube, and one was a malignant tubo-ovarian mass. All six cases were diagnosed the same on MRI and HPE.

Table 2: MRI diagnosis

MRI diagnosis	Number (30)	%
Serous cystadenoma	2	6.66
Mucinous cystadenoma	2	6.66
Serous cystadenocarcinoma	3	10
Mucinous cystadenocarcinoma	2	6.66
Solid benign ovarian tumors	4	13.33
Other carcinomas	4	13.33
Dermoid	2	6.66
Pedunculated/subserosal fibroid	1	3.33
Hemorrhagic cyst	3	10
Tubo-ovarian abscess	2	6.66
Simple ovarian cyst	2	6.66
Endometriosis	2	6.66
Indeterminate	1	3.33

The remaining five cases were indeterminate adnexal masses on USG, and further evaluation with MRI was recommended.

On MRI, out of the nineteen benign cases, eighteen cases were correctly diagnosed as benign lesions. One case was misdiagnosed as a benign mature cystic teratoma, which turned out to be a squamous cell carcinoma of the ovary on HPE.

In 25 cases (83.3%), both USG and MRI gave a similar diagnosis. MRI accurately diagnosed 4 indeterminate cases that correlated with the histopathology report.

One case was indeterminate even on MRI. Subsequent histopathological nature of the lesion revealed it to be a broad

ligament fibroid with non-visualization of the normal ovaries due to atrophy in a post-menopausal woman.

The nine malignant masses that were correctly diagnosed as malignant on MRI were three cases of serous cystadenocarcinoma, two cases of mucinous cystadenocarcinoma, one case of malignant tubo-ovarian mass, one case of endometrioid carcinoma, one case of serous papillary cystadenocarcinoma of the fallopian tube and two cases of malignant sex cord-stromal neoplasms.

Out of all the benign, the common lesions were hemorrhagic cysts (n=3). The characteristic appearance of the hemorrhagic cysts in ultrasound in the form of lace of lace-like reticular appearance in a cystic lesion with posterior acoustic enhancement and fluid-fluid level or intracystic clot with peripheral vascularity on CDFI on ultrasound and high signal intensity on both T1W and T2W MR images helps in inaccurate diagnosis of the lesions in both USG and MRI.

Next common benign lesions were serous cystadenomas, mucinous cystadenomas, and simple cysts(n=2).

Both the two simple cysts were diagnosed correctly on both ultrasound and MRI. The well defined thin wall and anechoic appearance with posterior acoustic enhancement and absence of internal septations or solid components within on ultrasound and well-defined lesions showing fluid signal intensity on all sequences without any internal septations or solid components help in the accurate diagnosis of these lesions on both ultrasound and MRI.

One case of serous cystadenoma was misinterpreted as an ovarian cyst by ultrasonography. MRI diagnosed it as serous cystadenoma due to its thin internal septations.

The other common benign lesion was mucinous cystadenoma (n=2), diagnosed by ultrasound and MRI because of its internal echoes and multilocular cystic lesion. There were no features of malignancy in both cases.

There were two cases of mucinous cystadenocarcinoma, which were accurately diagnosed as malignant on both USG and MRI due to the presence of solid components, mural thickening.

USG diagnosed two cases of solid malignant lesions.

There were three cases of tubo-ovarian abscesses out of which USG misdiagnosed one case of complex solid and cystic lesions as malignant. MRI diagnosed it as one case of a dermoid cyst.

USG and MRI accurately diagnosed one case of dermoid.

One case of the dermoid cyst was correctly diagnosed by both USG and MRI because of its hyperechoic fat content. On fat-sat MRI, the presence of fat was confirmed.

One case of pedunculated fibroid was misdiagnosed as a malignant ovarian lesion by USG. MRI diagnosed the ovaries separately and identified the origin.

Table 3: MRI for malignant lesions

Malignant	Disease		
	present	absent	
Positive	9	1	10
Negative	2	18	20
Total	11	19	30

There were five indeterminate cases (16.6%) by USG. For characterizing this malignant lesion, the sensitivity, specificity, and accuracy of MRI were identified as 81.80%, 94.7%, and 65.7%, and by USG the sensitivity, specificity, and accuracy were 36.6%, 94% and 55% respectively.

Table 4: Sensitivity and specificity of ultrasonography

USG diagnosis	Benign	Malignant
Sensitivity %	89.4	36.36
Specificity %	36.36	89.4
PPV %	89.4	66.66
NPV %	36.36	70.83
Accuracy %	27.5	52.5

Table 5: USG for malignant lesions

Malignant	Disease		
	present	absent	
Positive	4	1	5
Negative	7	18	24
Total	11	19	30

For characterizing the benign, the sensitivity, specificity, and accuracy of MRI were 94.7%, 90.0%, and 65%, and the sensitivity, specificity, and accuracy of USG were 94.7%, 90.9%, and 70%.

Table 6: Sensitivity and specificity of MRI diagnosis

Mri diagnosis	Benign	Malignant
Sensitivity %	94.7	81.8
Specificity %	90.0	94.7
PPV %	90.0	90.0
NPV %	90.0	90.0
Accuracy %	65.7	65.7

The best agreement was observed between MR findings and final diagnosis in origin, tissue content, and tissue characteristics. The common causes for sonographic indeterminate

masses were the location of the mass, solid appearance, and complex cystic appearance.

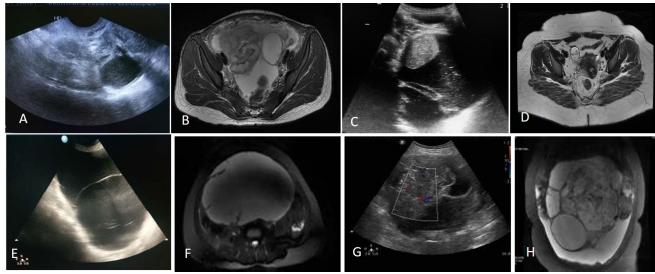


Figure 1: A. case 2. USG ABDOMEN: 23 Y old patient shows well defined cystic lesion with multiple thin internal echoes giving fishnet reticular appearance noted in the left ovary, s/o hemorrhagic cyst. B. case 2- MRI PELVIS: well-defined T2 hyperintense, T1 isointense lesion with few thin internal septations within occupying the entire left ovary. C. case.3. DERMOID CYST. USG Abdomen of a 38Y old patient shows a solid cystic lesion with cystic component showing internal echoes and a hyper-echoic solid focus, suggestive of fat. D. case 4-images showing a well-defined round to oval T1 hypointense and T2 hyperintense cystic lesion with a soft tissue attenuation component within, which demonstrates signal loss on FS sequence with the formation of fat fluid level in the right adnexa, s/o dermoid cyst. E. CASE 6: SEROUS CYSTADENOMA. USG ABDOMEN: A well defined cystic lesion meas. Approx. 20x17cm is noted in the pelvis extending into the abdomen with few thin internal septations within, no solid component/papillary projections probably epithelial adnexal neoplasm, mostly serous cystadenoma. F. case 6. MRI PELVIS: A large well defined T1 hypointense and T2 hyperintense cystic lesion meas. approx. 21x17.5cm noted in the pelvis extending into the abdomen with few thin internal septations within, no solid component/papillary projections probably epithelial adnexal neoplasm, mostly serous cystadenoma. G. CASE 9: MUCINOUS CYSTADENOCARCINOMA. USG of a 38Y old patient shows a well defined large mixed solid cystic lesion with multiple internal septations in the pelvis extending into the abdomen. Significant vascularity is noted in the solid component on CDFI. Probably epithelial ovarian neoplasm, mucinous cystadenocarcinoma. H. case 9. MRI PELVIS: showing a large well defined cystic lesion with multiple thin internal septations with the central solid component within noted in the midline of the abdomen. Multiple mixed is predominantly solid with cystic component lesions.

Discussion

The current study evaluated "The role of Ultrasonography and Magnetic Resonance Imaging in adnexal masses." Sensitivity, specificity, and accuracy of USG and MRI were correlated and compared.

In the present study, benign lesions (63.3%) were detected than malignant (36.6%), which is in concordance with Sohaib et al., where 60% had benign lesions, and 40% had malignant masses.^[7]

60% of all ovarian tumors and 85% of malignant ovarian neoplasms are ovarian epithelial neoplasms.^[6] Out of 30 cases, 19 cases were benign, and 11 cases were malignant.

In our study, Out of 30 cases, six cases were diagnosed as malignant in ultrasound. Out of these six cases, two were serious cystadenocarcinoma, two were mucinous cystadenocarcinoma, one was serious papillary cystadenocarcinoma of the fallopian tube, and one was a malignant tubo-ovarian mass. All six cases were diagnosed the same on MRI and HPE. The remaining five cases were indeterminate adnexal masses on USG, and further evaluation with MRI was recommended. On MRI, out of the nineteen benign cases, eighteen cases were correctly diagnosed as benign lesions. One case was misdiagnosed as a benign mature cystic teratoma, which turned out to be a squamous cell carcinoma of the ovary on HPE.

Our study reveals that although USG is the first line of investigation for uterine fibroids, it performs poorly in determining the origin of the mass, which is the essential first step in characterizing the pelvic mass.

MRI characterized both lesions accurately because of its hypointense signal intensity on the T2W image.

There were five indeterminate cases (16.6%) in this study, diagnosed accurately by MRI. This was similar to Hricak H et al. wherein 20% of adnexal lesions were classified as indeterminate by USG.^[8]

The best agreement was observed between MR findings and the final diagnosis. Sonography had a relatively weak correlation in context to the definitive diagnosis for the origin and tissue content of a mass.

In our study, MRI showed more specific and accurate than ultrasonography to characterize adnexal masses. This was in concordance to Allen et al., where MRI was more specific and accurate than Ultrasonography.

Our study also shows that a high detection rate and accurate characterization of the adnexal lesions are possible using MRI, similar to a study conducted by Sohaib et al.

Unenhanced T1 and T2 weighted imaging are essential for accurate tissue characterization. Lipid and blood products are readily detected on T1 WI with or without fat suppression. T2 WI helps to identify the low signal intensity of fibrous tissue.

MRI correctly revealed the tissue content of all masses except a functional ovarian cyst that was thought to have cystic and solid components. MRI was shown to have excellent agreement with the final diagnosis for identifying specific tissue characteristics (fat, hemorrhage, fibrous and leiomyomatosis tissue). This enabled the accurate diagnosis of dermoid, hemorrhagic cysts, endometriomas, uterine fibroids, and fibrous tumors of the ovary.

Conclusion

The ability of MRI to manipulate tissue contrast makes this technique an invaluable tool in the assessment of complex adnexal masses, helping in the characterization of such masses. MRI is more specific and accurate than USG for characterising adnexal masses due to better soft-tissue resolution and multiplanar imaging. MRI was helpful to detect the malignant potential of a particular lesion and hence plays the role in oncological staging. USG is sensitive in picking up lesions and helps as an initial imaging modality for the screening of adnexal lesions and is the main triage method before treatment. MRI helps in the evaluation of indeterminate cases.

References

1. Adusumilli S, Hussain HK, Caoili EM, Weadock WJ, Murray JP, Johnson TD, et al. MRI of Sonographically Indeterminate Adnexal Masses. *Am J Roentgenol.* 2006;187(3):732–740. Available from: <https://dx.doi.org/10.2214/ajr.05.0905>.
2. Sohaib SAA, Sahdev A, Trappen PV, Jacobs IJ, Reznick RH. Characterization of Adnexal Mass Lesions on MR Imaging. *Am J Roentgenol.* 2003;180(5):1297–1304. Available from: <https://dx.doi.org/10.2214/ajr.180.5.1801297>.
3. Agostinho L, Cruz R, Osório F, Alves J, Setúbal A, Guerra A. MRI for adenomyosis: a pictorial review. *Insights Imaging.* 2017;8(6):549–556. Available from: <https://dx.doi.org/10.1007/s13244-017-0576-z>.
4. Siegelman ES, Body M. Elsevier saunders publications;
5. Scout LM, Flynn SD. Junctional zone of the cervix: correlation of MR imaging and histologic examination of hysterectomy specimens. *Radiology.* 1993;186:159–62. Available from: <https://doi.org/10.1148/radiology.179.2.2014282>.
6. Saini A, Dina R, McIndoe GA, Soutter WP, Gishen P, deSouza NM. Characterization of Adnexal Masses with MRI. *Am J Roentgenol.* 2005;184(3):1004–1009. Available from: <https://dx.doi.org/10.2214/ajr.184.3.01841004>.
7. Sohaib SA, Mills TD, Sahdev A, Webb JAW, VanTrappen PO, Jacobs IJ, et al. The role of magnetic resonance imaging and ultrasound in patients with adnexal masses. *Clin Radiol.* 2005;60(3):340–348. Available from: <https://dx.doi.org/10.1016/j.crad.2004.09.007>.
8. Hricak H, Chen M, Coakley FV, Kinkel K, Yu KK, Sica G, et al. Complex Adnexal Masses: Detection and Characterization with MR Imaging—Multivariate Analysis. *Radiology.* 2000;214:39–46. Available from: <https://dx.doi.org/10.1148/radiology.214.1.r00ja3939>.

Copyright: © the author(s), 2020. It is an open-access article distributed under the terms of the Creative Commons Attribution License (CC BY 4.0), which permits authors to retain ownership of the copyright for their content, and allow anyone to download, reuse, reprint, modify, distribute and/or copy the content as long as the original authors and source are cited.

How to cite this article: Nitya N, Baru RKR. Comparative Study of Ultrasound and Magnetic Resonance Imaging of Adnexal Masses. *Asian J. Med. Radiol. Res.* 2020;8(2):106-111.

DOI: dx.doi.org/10.47009/ajmrr.2020.8.2.17

Source of Support: Nil, **Conflict of Interest:** None declared.